THE JOURNAL OF PHYSICAL CHEMISTRY Letters

pubs.acs.org/JPCL Letter

Probing the Microsolvation Environment of the Green Fluorescent Protein Chromophore *In Vacuo*

Wyatt Zagorec-Marks, Madison M. Foreman, Jan R. R. Verlet, and J. Mathias Weber*

Cite This: *J. Phys. Chem. Lett.* 2020, 11, 1940−1946 Read Online

ACCESS | Metrics & More | Article Recommendations | Supporting Information

ABSTRACT: We present vibrational and electronic photodissociation spectra of a model chromophore of the green fluorescent protein in complexes with up to two water molecules, prepared in a cryogenic ion trap at 160−180 K. We find the band origin of the singly hydrated chromophore at 20 985 cm^{-1} (476.5 nm) and observe partially resolved vibrational signatures. While a single water molecule induces only a small shift of the S_1 electronic band of the chromophore, without significant change of the Franck−Condon envelope, the spectrum of the dihydrate shows significant broadening and a greater blue shift of the band edge. Comparison of the vibrational spectra with predicted infrared spectra from density functional theory indicates that water molecules can interact with the oxygen atom on the phenolate group or on the imidazole moiety, respectively.

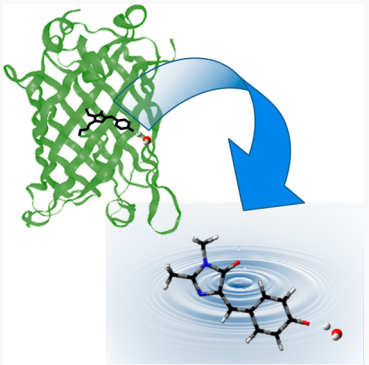

Many proteins incorporate water molecules as a part of their functional structure.[1,2] As a result, microsolvation is an important structural aspect that influences the properties of functional regions in proteins. For example, in many fluorescent proteins, such as those based on the green fluorescent protein (GFP), a water molecule binds to the anionic phenolate group of the chromophore that is situated within the double-barrel protein structure.[3] The influence of the water molecule on the photophysics of the chromophore is therefore of great interest. One way of probing water−chromophore interactions is to use a model chromophore, which in GFP is a small anion consisting of a phenolate group connected by a methine bridge at the para-position to an imidazole group. This chromophore is represented very well by deprotonated *p*-hydroxybenzylidene-2,3-dimethylimidazolinone ($HBDI^-$, see Supporting Information, Scheme S1), where the two methyl groups on the imidazole moiety replace the connections to the protein. The addition of water molecules to this chromophore can alter its electronic structure, and such changes should be reflected in the absorption spectrum of the chromophore. The $S_1 \leftarrow S_0$ absorption spectrum of $HBDI^-$ in aqueous solution is strongly blue-shifted from that of the protein, as the peak absorption changes from ca. 480 nm to ca. 426 nm.[4] In contrast, the photodissociation spectrum of $HBDI^-$ *in vacuo* bears a striking resemblance to the absorption spectrum of GFP, which can be observed in even more detail for cryogenically prepared $HBDI^-$ and GFP at 77 K, with a blue shift in the protein by just 300 cm^{-1}.[4−6] The comparison suggests that the interactions with the protein environment, including neighboring charged residues and the water in the chromophore pocket, bring the electronic structure of the chromophore closer to vacuum than to aqueous solution. Consequently, there has been much interest in the photophysics of $HBDI^-$ *in vacuo* over the past two decades.[4,6−32] However, the influence of water−$HBDI^-$ interaction on the electronic spectrum of the chromophore has so far only been investigated computationally.[13] One of the questions in this context is whether the water molecule in the chromophore pocket of GFP has a strong influence on the electronic spectrum of the chromophore, which would then have to be countered by the rest of the interactions in the pocket.

In this work, we present vibrational and electronic spectroscopy of mass selected clusters of $HBDI^-$ with up to two water molecules that have been cryogenically prepared in an ion trap. We show that in the absence of the constraints imposed by the chromophore pocket, water molecules can bind to the phenolate or to the oxygen on the imidazole moiety, and we can clearly distinguish between the two binding sites in the vibrational spectrum.

Figure 1 shows the photodissociation spectra of the $S_1 \leftarrow S_0$ absorption band of $HBDI^-\cdot(H_2O)_n$ (n = 1, 2) at 160−180 K, compared to the spectrum of bare $HBDI^-$ taken at 30 K trap temperature[6] (see Supporting Information for experimental and computational methods). The overall shapes of the spectra for $HBDI^-$ and $HBDI^-\cdot H_2O$ are nearly identical. The

Received: January 10, 2020
Accepted: February 19, 2020
Published: February 19, 2020

https://dx.doi.org/10.1021/acs.jpclett.0c00105
J. Phys. Chem. Lett. 2020, 11, 1940−1946

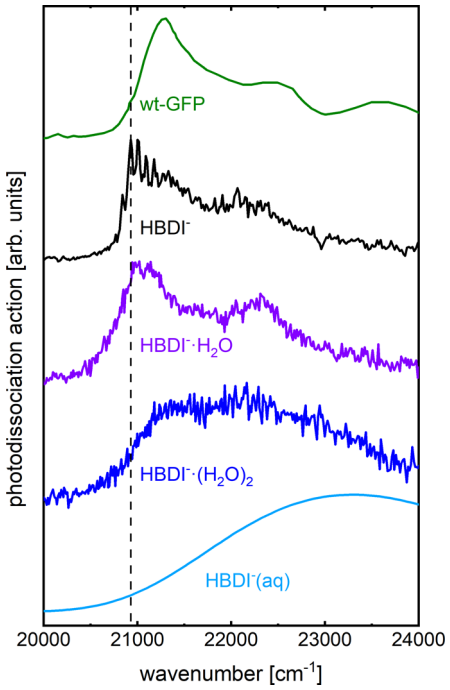

Figure 1. From top: Absorption spectrum of wild-type GFP at 77 K (green); photodissociation spectra of $HBDI^-$ at 30K (black) and $HBDI^-\cdot(H_2O)_n$ (n = 1, 2, magenta and blue) in the visible spectral region; UV/vis absorption spectrum of aqueous $HBDI^-$ at pH 11 (light blue). All traces were normalized to the same peak height. Photofragment signals were the loss of a methyl group for bare $HBDI^-$ and of all H_2O molecules for $HBDI^-\cdot(H_2O)_n$, respectively. The vertical dashed line marks the band origin of bare $HBDI^-$ at 20 930 cm^{-1}. The data for bare $HBDI^-$ were taken from ref 6, and the absorption spectrum of wild-type GFP was digitized from ref 5.

vibrational features in the Franck–Condon profile of the spectrum of the monohydrate are less well resolved than for bare $HBDI^-$, but we assign the band origin to a partially resolved peak at (20 985 ± 30) cm^{-1}, representing a 55 cm^{-1} blue shift from bare $HBDI^-$. Additional vibrational features are a partially resolved peak at ca. 21 120 cm^{-1} and a shoulder at 21 195 cm^{-1}. These features are likely the remnants of the Franck–Condon progression in a low-frequency bending vibration of the methine bridge.[6] We assign the set of peaks around 22 200 cm^{-1} to an imidazole ring breathing/in-plane CH bending mode and its combination bands with the aforementioned methine bridge bending mode.[6,9,12,33] While the addition of a single water molecule does not seem to cause much change in the electronic spectrum of $HBDI^-$, the spectrum of the dihydrate shows a significantly altered envelope, with a broad feature around 21 400 cm^{-1}, followed by another around 22 130 cm^{-1}. We cannot extract a clean band origin from the spectrum, but we find that the half-maximum point on the rising edge of the first feature is blue-shifted by ca. 180 cm^{-1} from the analogous point in the spectrum of the monohydrate. A better understanding of the effects of hydration on the properties of $HBDI^-$ requires a detailed structural characterization of the clusters studied here.

We begin the structural characterization of $HBDI^-\cdot(H_2O)_n$ (n = 1, 2) clusters by determining which isomer of $HBDI^-$ is present, as the chromophore can exist in two different isomeric forms denoted E and Z (see Scheme S1 in Supporting Information), which are connected by torsion around the methine bridge. Both of these isomers are encountered in proteins, but only the Z isomer is fluorescent (present in GFP), while the E isomer is not.[34,35] We recently used IR spectroscopy to establish that the Z isomer is the dominant species if prepared at low temperatures (30 K), in complexes with weakly bound N_2 messenger tags.[6] In the present experiment, we formed $HBDI^-\cdot(H_2O)_n$ clusters by condensing water molecules from the background gas of the vacuum apparatus onto $HBDI^-$ at trap temperatures of 160–180 K. Figure 2 shows the infrared fingerprint region of the $HBDI^-$

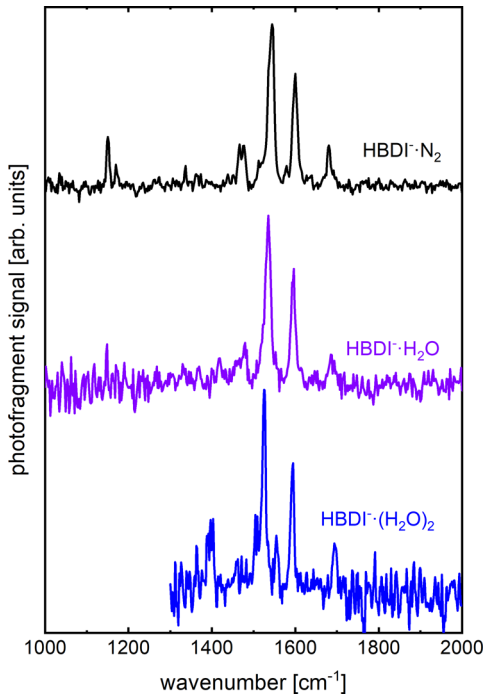

Figure 2. Infrared photodissociation spectra of $HBDI^-\cdot N_2$ and $HBDI^-\cdot(H_2O)_n$ (n = 1, 2) in the fingerprint region of $HBDI^-$ vibrations. The photofragment signals were due to the loss of N_2 for $HBDI^-\cdot N_2$ and of a single H_2O molecule for $HBDI^-\cdot(H_2O)_n$, respectively. The spectrum of $HBDI^-\cdot N_2$ was taken from ref 6.

vibrations for $HBDI^-\cdot(H_2O)_n$ (n = 1, 2) compared to that of $HBDI^-\cdot N_2$, which we previously reported and assigned to the Z isomer.[6] Our assignment of the infrared spectrum to the Z isomer relies primarily on the spacing of the three intense features around 1600 cm^{-1}. Based on the comparison in Figure 2, we determine that the Z isomer is dominant in the water complexes, consistent with ion mobility results reported by Bieske and coworkers[30] where solvent complexes (with methanol in their work) only existed for the Z isomer.

The positions of the most intense vibrational signatures of $HBDI^-\cdot N_2$ shown in Figure 2 are only weakly influenced by the microsolvation environment (by up to ca. 10 cm^{-1} per water molecule, see Supporting Information, Table S1), showing a minor influence of the water adducts on the robust $HBDI^-$ frame, in line with computational predictions by Krylov and coworkers.[13] The observed changes in vibrational frequencies are likely due to small changes in the charge distribution that results from water molecules binding to either of the oxygen atoms (see Supporting Information, Table S2). Some of the observed changes suggest that hydration occurs on the phenolate moiety; for example, a slight blue shift observed for the imidazole CO stretching vibration found in $HBDI^-\cdot N_2$ at ca. 1680 cm^{-1}, and the enhancement of a

https://dx.doi.org/10.1021/acs.jpclett.0c00105
J. Phys. Chem. Lett. 2020, 11, 1940–1946

phenolate CO stretching signature at 1396 cm^{-1} in the dihydrate spectrum. However, a weak band around 1650 cm^{-1} is consistent with hydration on the imidazole, so we can expect a mixture of conformers to be present. A more detailed discussion of the vibrational spectrum in the fingerprint region of $HBDI^-\cdot(H_2O)_n^-$ and comparison with predicted spectra for various hydration conformers is given in Supporting Information.

While the fingerprint region (1000−2000 cm^{-1}) shows the (weak) effects of microhydration on the solute, the OH stretching region encodes microhydation from the solvent point of view, and presents a clearer picture, as the OH stretching frequencies of the water molecules are highly sensitive probes of their hydrogen bonding environment. Figure 3 shows the experimental infrared spectra of $HBDI^-\cdot N_2$,

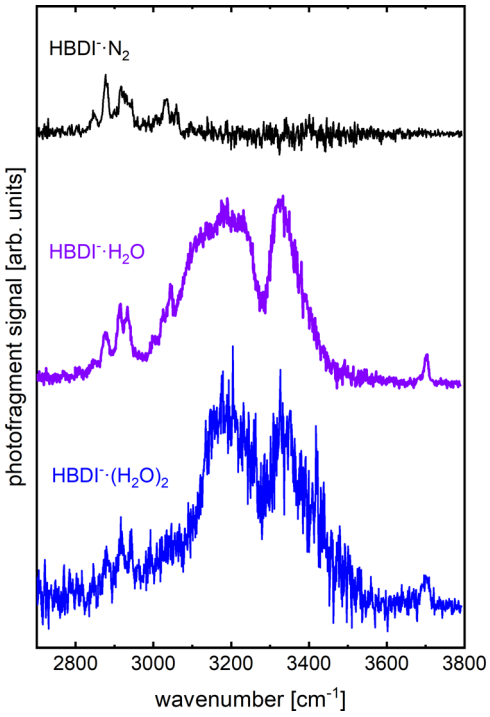

Figure 3. Infrared photodissociation spectra of $HBDI^-\cdot N_2$ (top, black) and $HBDI^-\cdot(H_2O)_n$ (n = 1, 2, magenta and blue) from 2700 to 3800 cm^{-1}. The photofragment signals were the loss of N_2 and a single H_2O molecule for $HBDI^-\cdot N_2$ and $HBDI^-\cdot(H_2O)_n$, respectively.

and of the mono- and dihydrate of $HBDI^-$ over the range of 2700−3800 cm^{-1}. The spectra of $HBDI^-\cdot(H_2O)_n$ are dominated by broad features in the region of 3100−3500 cm^{-1}, which contain the signatures of the hydrogen bonded (H-bonded) OH groups of the water molecules. The free OH signature appears at 3703 cm^{-1}. In the range of 2800−3100 cm^{-1}, the spectrum of $HBDI^-\cdot N_2$ carries the signatures of the CH stretching vibrational modes, which are also observed in the spectra of the hydrated ions (see Supporting Information for a more detailed discussion of the CH stretching modes).

Figure 4 shows a comparison of the experimental and simulated infrared spectra for several calculated conformers of the monohydrate complex, $HBDI^-\cdot H_2O$. We assign the broad feature around 3180 cm^{-1} to the signature of the symmetric stretching mode of a water molecule solvating the phenolate group (conformer Ia), which is largely localized on the OH group H-bonded to the ion. There is an analogous conformer

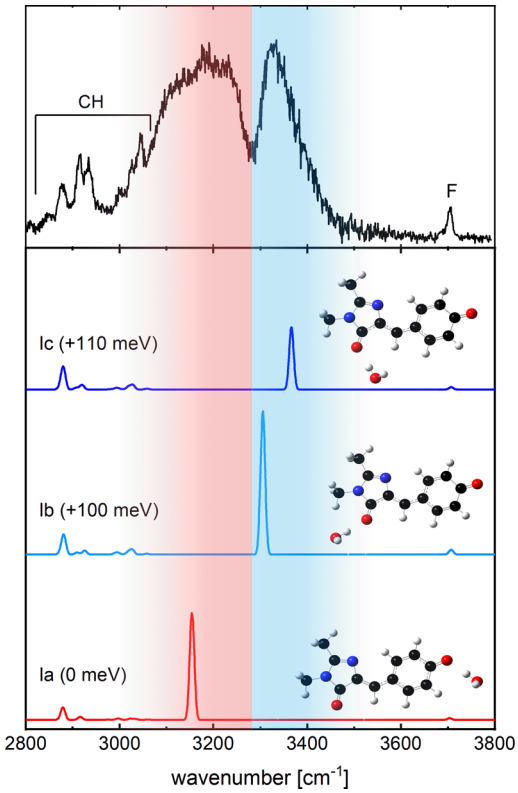

Figure 4. Calculated infrared spectra of several conformers of monohydrated $HBDI^-$ (lower traces), compared to the experimental spectrum (upper trace). The spectrum contains signatures for CH stretching vibrations (CH), H-bonded OH stretching on the phenolate (red-shaded region) and imidazole (blue-shaded region) groups, and the free OH stretching mode (F). All calculations have been scaled by 0.957 to match the experimentally observed free OH stretching vibrations. The calculated energies (at 0 K) of the conformers relative to the lowest energy conformer (Ia) are given in each simulated trace.

(Ia′, see Supporting Information, Figure S1) *anti* to the methine bridge CH group, which is isoenergetic (within 5 meV) with conformer Ia and has the same infrared spectrum. The feature around 3340 cm^{-1} carries the signature of a water molecule solvating the imidazole oxygen (conformers Ib and Ic). The observation of both features in the spectrum of $HBDI^-\cdot H_2O$ shows that a mixture of the two hydration conformers is present in the experiment. The two conformers for hydration at the imidazole (Ib and Ic) are separated by a barrier of ca. 40 meV. The widths of the infrared bands reflect the fact that the complexes are formed through an evaporative ensemble,[36] with internal energies of the order of the binding energy of a water molecule (see discussion below). As a result, the water molecule is likely to explore a significant range of $OH\cdots O^-$ angles through large amplitude motions, both in the plane of the $HBDI^-$ ion and perpendicular to it, and this motion results in broadening of the corresponding OH stretching transitions (see Supporting Information).

Overall, we obtain similar structures and energetic ordering as found by Krylov and coworkers.[13] The lowest energy structure of the monohydrate corresponds to hydration on the phenolate (structure Ia). Hydration on the imidazole is ca. 100 meV higher in energy, where the oxygen lone pair of the water molecule can be weakly tethered to the nearest methyl group (structure Ib) or to the CH group on the methine bridge (Ic,

https://dx.doi.org/10.1021/acs.jpclett.0c00105
J. Phys. Chem. Lett. 2020, 11, 1940−1946

the only imidazole-binding structure reported by Krylov and coworkers[13]). Conformers Ib and Ic have different OH stretching frequencies, and the geometries sampled by large amplitude motion connecting the two structures will contribute to the broadening of the OH stretching feature of the OH group H-bonded to the imidazole (see Supporting Information).

To obtain a coarse estimate of relative populations for the two hydration sites, we fitted the two H-bonded OH features with Gaussian profiles and compared the peak areas scaled by the calculated infrared intensities for conformers Ia and Ib. The result suggests that in ca. 60% of the complexes the water molecule is bound to the phenolate, and ca. 40% have a hydrated imidazole structure. Interestingly, the estimated population ratio of the two conformers is not consistent with a thermal population. In principle, the different binding energies of the water molecules to the different binding sites could lead to overestimating the imidazole population by suppressing photodissociation from the more strongly bound conformers. The binding energy at the imidazole site (calculated at 3740 cm^{-1}) is less than at the phenolate (calculated at 4550 cm^{-1}). However, there is considerable energy in the complexes, since they are formed in the ion trap from an evaporative ensemble.[36] The energy in a complex formed this way is of the order of the binding energy of a water molecule in the dihydrate, which is calculated to be between 3300 and 4500 cm^{-1}. As a result, the internal energy in the complex assists in dissociation after photon absorption. This is also evidenced by the fact that we can record infrared photodissociation spectra in the carbonyl stretching region (see Figure 2). To explain the estimated population ratio, we assume that water migration between the two binding sites is hindered by a large barrier, leading to kinetically trapped species. We hypothesize that the formation of the two different hydration conformers can be better described by cross sections for the capture of a water molecule in the ion trap by the two different binding sites of $HBDI^-$. We note that future experiments that could employ separation of water adduct formation and messenger tagging[37] together with hole-burning spectroscopy[38,39] could allow the observation and assignment of individual hydration conformers.

The spectrum of the dihydrate in the OH stretching region is quite similar to that of the monohydrate. It is dominated by a broad feature around 3190 cm^{-1} and a second broad feature around 3340 cm^{-1}. The two water molecules can be either H-bonded to the same oxygen, or one can each be bonded to the two binding sites, resulting in three possible binding site occupation combinations. There are several conformers for the same occupation of binding sites, since there is some conformational flexibility within each binding site, and these conformers are close in energy. Figure 5 shows a comparison of calculated infrared spectra for several conformers with the experimental spectrum.

Conformer IIa is the lowest energy conformer (at 0 K), with both water molecules binding to the phenolate, and forming a water−water H-bond. Note, however, that the experimental spectrum does not show any feature that would indicate that the two water molecules form a water−water H-bond, which is predicted at ca. 3600 cm^{-1}. Experiments by Johnson and coworkers on $I^-\cdot(H_2O)_2$ demonstrated that the water−water H-bond in that cluster does not survive at the trap temperatures in the present experiment, easily explaining the absence of the water−water H-bond signature.[40] Based on

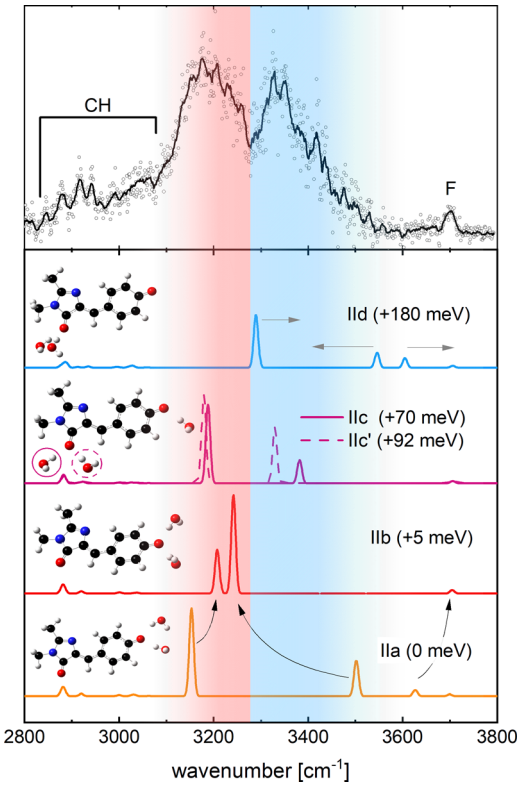

Figure 5. Calculated infrared spectra of several conformers of $HBDI^-\cdot(H_2O)_2$ (lower traces), compared to the experimental spectrum (upper trace). The points in the upper trace are raw data; the full black line is an 11-point gliding average to guide the eye. The spectrum contains signatures for CH stretching vibrations (CH), OH stretching H-bonded to the phenolate (red-shaded region) and imidazole (blue-shaded region) groups, and the free OH stretching mode (F). All calculations have been scaled by 0.957 to match the experimentally observed free OH stretching vibrations. The calculated energies (at 0 K) of the conformers relative to the lowest energy conformer (IIa) are given in each simulated trace. Arrows in the lowest trace show how the infrared features of conformer IIa change as the H-bond between the water molecules is lost (see text). Arrows in the trace for conformer IId show the expected analogous behavior upon breaking the water−water H-bond for a conformer with both water molecules on the imidazole. The full and dashed lines in the trace for conformers IIc and IIc′ correspond to the water molecule positions indicated by full and dashed circles, respectively.

their work, we expect the two ionic H-bond signatures to shift closer together, concomitant with breaking the water−water H-bond, behaving like independent monomers rather than dimers. The corresponding conformer (IIb) in the present case is in fact a stable minimum energy structure, which is practically isoenergetic with conformer IIa. At the internal energies of the complexes, the significantly higher entropy of conformer IIb will drive breaking the water−water H-bond, and we expect that conformer IIa is not in fact populated at this temperature. As a result, the lower frequency feature in the experimental spectrum is still indicative of hydration on the phenolate (conformers IIa, IIb), while the higher frequency feature signals hydration on the imidazole (conformers IIc, IIc′, IId). We note that at 0 K, there is no minimum energy structure with two independent water molecules at the imidazole. However, we still expect the same entropy driven loss of the water−water H-bond to occur for this hydration configuration, with the concomitant behavior of the calculated

https://dx.doi.org/10.1021/acs.jpclett.0c00105
J. Phys. Chem. Lett. 2020, 11, 1940−1946

infrared signatures of conformer IId indicated by the arrows shown in Figure 5.

The observed dihydrate spectrum is consistent with a mixture of conformers corresponding to doubly and two singly hydrated binding sites, but due to the multitude of different conformers, we refrain from estimating the population ratio of the different conformers here. The free OH signature in the dihydrate spectrum is broader than in the monohydrate spectrum, reflecting the composition of the spectrum from several hydration conformers with slightly varying free OH frequencies. The relative energies for the dihydrate favor hydration of the phenolate by both water molecules, followed by one water molecule on each binding site (ca. 70 meV higher in energy), with two water molecules on the imidazole being highest in energy (ca. 180 meV above dihydrated phenolate), in line with calculations by Krylov and coworkers.[13]

With our insight into the structures of hydrated $HBDI^-$, we can return to the electronic spectra of these clusters. Calculations by Krylov and coworkers[13] at the SOS-CIS(D)/cc-pVTZ level predict a blue shift of 240 cm^{-1} for hydration at the phenolate moiety and a red shift by 160 cm^{-1} for hydration at the imidazole group. Our calculations, done at the CAM-B3LYP/def2-TZVPP level of theory, suggest a 9 cm^{-1} red shift and a 54 cm^{-1} blue shift for hydration at the phenolate and imidazole, respectively. Based on the experimental electronic spectrum of cryogenically prepared $HBDI^-$, the vertical excitation energies are equal to the band origin energies in the Franck–Condon region, which represents a shallow minimum on the S_1 potential energy surface.[6] We assume that the first feature in the monohydrate spectrum at 20 985 cm^{-1}, which is broader than the band origin feature for bare $HBDI^-$, contains the band origins of both hydration conformers. The splitting between the band origins of the two hydration conformers in our calculations is quite close to the experimentally observed width of this feature, although the good agreement is likely to be fortuitous. The splitting calculated by the Krylov group[13] (400 cm^{-1}) is too large to maintain the experimentally observed width of the Franck–Condon profile. It is worth comparing the small blue shift upon hydration with the blue shift caused by betaine, an adduct with a much stronger dipole moment.[31] The shift induced by betaine (ca. 12 D dipole moment[31]) is 640 cm^{-1}, while the shift induced by water (1.85 D dipole moment) is 55 cm^{-1}, i.e., the shift introduced by water is even lower (by a factor of 1.8) than expected based on the electric field of betaine.

The calculated vertical excitation energies for the three hydration conformer families of the dihydrate span ca. 300 cm^{-1}, and several of the conformers exhibit a red shift (see Supporting Information, Table S3). These calculations do not explain the blue shift of the spectrum or the deviation from the characteristic band envelope found in $HBDI^-{\cdot}N_2$ and $HBDI^-{\cdot}H_2O$. Previous calculations by Krylov and coworkers[13] arrived at a difference of 960 cm^{-1} between the different hydration conformers for the dihydrate, which could lead to a change in the observed band shape. We hypothesize that the change observed in the envelope of dihydrate spectrum is indeed caused by a mixture of different hydration conformers. However, in light of the complications arising from the mix of hydration conformers and the lack of clear computational description, we refrain from a more definitive assignment. Clearly, the currently available calculations are not able to satisfactorily explain the dihydrate spectrum, particularly its significant blue shift compared to that of the monohydrate. We note that the larger effect of the second water molecule is unexpected, since most often the first one or two water molecules each introduce a significant shift, while additional water adducts result in less dramatic changes.[41,42] This is clearly not the case here, where the second water adduct brings the spectrum much closer to bulk solution than the first (see Figure 1). Future work with larger hydrated clusters could shed light on the transition to full hydration.

In summary, clusters of $HBDI^-$ with up to two water molecules are based on the *Z* isomeric form of the chromophore itself. There are two binding sites for water molecules in $HBDI^-$, the oxygen atoms on the phenolate and the imidazole moieties, respectively, and we observe hydration on both. For the monohydrate, the relative population on each binding site cannot be described by thermal conformer distributions, and we assume that the populations are given by capture of a water molecule into either binding site and subsequent cooling and kinetic trapping. The dihydrate shows a mixture of hydration conformers, and at the range of trap temperatures in the present work, we do not find the signatures of water–water hydrogen bonding. In contrast to the dihydrate, whose electronic spectrum envelope deviates from that of bare $HBDI^-$, a single water molecule interacting with $HBDI^-$ does not significantly change the envelope of the $S_1 \leftarrow S_0$ electronic band, and the shift of the band origin from bare $HBDI^-$ is only +55 cm^{-1}. In the context of interpreting $HBDI^-$ as a model for the GFP chromophore, this observation implies that the ca. 300 cm^{-1} shift caused by the chromophore environment is not caused by the functional water molecule that binds to the phenolate moiety in the protein.

■ ASSOCIATED CONTENT

Supporting Information

The Supporting Information is available free of charge at https://pubs.acs.org/doi/10.1021/acs.jpclett.0c00105.

Isomers of $HBDI^-$; experimental and computational methods; vibrational assignments for $HBDI^-{\cdot}N_2$ and $HBDI^-{\cdot}(H_2O)_n$ (n = 1, 2) in the fingerprint region; calculated selected charges and bond lengths in $HBDI^-$ and different position isomers for $HBDI^-{\cdot}(H_2O)_n$ (n = 1, 2); calculated vertical excitation energies for all structures; discussion of the influence of water adducts on the fingerprint region of $HBDI^-$ vibrational modes; comparison of calculated and experimental infrared spectra of $HBDI^-{\cdot}(H_2O)_n$ (n = 1, 2) from 1350 to 1800 cm^{-1}; calculated hydrogen bonded OH stretching frequency as a function of hydration geometry in $HBDI^-{\cdot}H_2O$ in the plane of $HBDI^-$; calculated hydrogen bonded OH stretching frequency as a function of hydration geometry in $HBDI^-{\cdot}H_2O$ perpendicular to the plane of $HBDI^-$; discussion of CH stretching modes; all calculated structures with atomic coordinates and frequencies (PDF)

■ AUTHOR INFORMATION

Corresponding Author

J. Mathias Weber − *JILA and Department of Chemistry, University of Colorado, Boulder, Colorado 80309-0440, United States;* orcid.org/0000-0002-5493-5886; Phone: +1-303-492-7841; Email: weberjm@jila.colorado.edu

https://dx.doi.org/10.1021/acs.jpclett.0c00105
J. Phys. Chem. Lett. 2020, 11, 1940−1946

Authors

Wyatt Zagorec-Marks − *JILA and Department of Chemistry, University of Colorado, Boulder, Colorado 80309-0440, United States*

Madison M. Foreman − *JILA and Department of Chemistry, University of Colorado, Boulder, Colorado 80309-0440, United States*

Jan R. R. Verlet − *Department of Chemistry, Durham University, Durham DH1 3LE, U.K.;* orcid.org/0000-0002-9480-432X

Complete contact information is available at: https://pubs.acs.org/10.1021/acs.jpclett.0c00105

Notes

The authors declare no competing financial interest.

■ ACKNOWLEDGMENTS

We gratefully acknowledge support from the U.S. National Science Foundation under award no. CHE-1764191, the NSF Physics Frontier Center at JILA (award no. PHY-1734006), and JILA for a Visiting Fellowship to J.R.R.V. We also thank Drs. Stephen R. Meech and Philip C. B. Page (University of East Anglia, U.K., grant support through EPSCR grants EP/E010466 and EP/H025715) for providing us with the *p*-hydroxybenzylidene-2,3-dimethylimidazolinone samples that were used in this work.

■ REFERENCES

(1) Genick, U. K.; Soltis, S. M.; Kuhn, P.; Canestrelli, I. L.; Getzoff, E. D. Structure at 0.85-Å Resolution of an Early Protein Photocycle Intermediate. *Nature* **1998**, *392*, 206−209.

(2) Moukhametzianov, R.; Klare, J. P.; Efremov, R.; Baeken, C.; Göppner, A.; Labahn, J.; Engelhard, M.; Büldt, G.; Gordeliy, V. I. Development of the Signal in Sensory Rhodopsin and Its Transfer to the Cognate Transducer. *Nature* **2006**, *440*, 115−119.

(3) Ormö, M.; Cubitt, A. B.; Kallio, K.; Gross, L. A.; Tsien, R. Y.; Remington, S. J. Crystal Structure of the Aequorea Victoria Green Fluorescent Protein. *Science* **1996**, *273*, 1392−1395.

(4) Nielsen, S. B.; Lapierre, A.; Andersen, J. U.; Pedersen, U. V.; Tomita, S.; Andersen, L. H. Absorption Spectrum of the Green Fluorescent Protein Chromophore Anion in Vacuo. *Phys. Rev. Lett.* **2001**, *87*, 228102.

(5) Chattoraj, M.; King, B. A.; Bublitz, G. U.; Boxer, S. G. Ultra-Fast Excited State Dynamics in Green Fluorescent Protein: Multiple States and Proton Transfer. *Proc. Natl. Acad. Sci. U. S. A.* **1996**, *93*, 8362−8367.

(6) Zagorec-Marks, W.; Foreman, M. M.; Verlet, J. R. R.; Weber, J. M. Cryogenic Ion Spectroscopy of the Green Fluorescent Protein Chromophore in Vacuo. *J. Phys. Chem. Lett.* **2019**, *10*, 7817−7822.

(7) Andersen, L. H.; Lapierre, A.; Nielsen, S. B.; Nielsen, I. B.; Pedersen, S. U.; Pedersen, U. V.; Tomita, S. Chromophores of the Green Fluorescent Protein Studied in the Gas Phase. *Eur. Phys. J. D* **2002**, *20*, 597−600.

(8) Forbes, M. W.; Jockusch, R. A. Deactivation Pathways of an Isolated Green Fluorescent Protein Model Chromophore Studied by Electronic Action Spectroscopy. *J. Am. Chem. Soc.* **2009**, *131*, 17038−17039.

(9) Martin, M. E.; Negri, F.; Olivucci, M. Origin, Nature, and Fate of the Fluorescent State of the Green Fluorescent Protein Chromophore at the CASPT2//CASSCF Resolution. *J. Am. Chem. Soc.* **2004**, *126*, 5452−5464.

(10) Chingin, K.; Balabin, R. M.; Frankevich, V.; Barylyuk, K.; Nieckarz, R.; Sagulenko, P.; Zenobi, R. Absorption of the Green Fluorescent Protein Chromophore Anion in the Gas Phase Studied by a Combination of FTICR Mass Spectrometry with Laser-Induced Photodissociation Spectroscopy. *Int. J. Mass Spectrom.* **2011**, *306*, 241−245.

(11) Forbes, M. W.; Nagy, A. M.; Jockusch, R. A. Photofragmentation of and Electron Photodetachment from a GFP Model Chromophore in a Quadrupole Ion Trap. *Int. J. Mass Spectrom.* **2011**, *308*, 155−166.

(12) Kamarchik, E.; Krylov, A. I. Non-Condon Effects in the One- and Two-Photon Absorption Spectra of the Green Fluorescent Protein. *J. Phys. Chem. Lett.* **2011**, *2*, 488−492.

(13) Zuev, D.; Bravaya, K. B.; Makarova, M. V.; Krylov, A. I. Effect of Microhydration on the Electronic Structure of the Chromophores of the Photoactive Yellow and Green Fluorescent Proteins. *J. Chem. Phys.* **2011**, *135*, 194304.

(14) Almasian, M.; Grzetic, J.; Berden, G.; Bakker, B.; Buma, W. J.; Oomens, J. Gas-Phase Infrared Spectrum of the Anionic GFP-Chromophore. *Int. J. Mass Spectrom.* **2012**, *330*, 118−123.

(15) Horke, D. A.; Verlet, J. R. R. Photoelectron Spectroscopy of the Model GFP Chromophore Anion. *Phys. Chem. Chem. Phys.* **2012**, *14*, 8511−8515.

(16) Mooney, C. R. S.; Sanz, M. E.; McKay, A. R.; Fitzmaurice, R. J.; Aliev, A. E.; Caddick, S.; Fielding, H. H. Photodetachment Spectra of Deprotonated Fluorescent Protein Chromophore Anions. *J. Phys. Chem. A* **2012**, *116*, 7943−7949.

(17) Toker, Y.; Rahbek, D. B.; Klaerke, B.; Bochenkova, A. V.; Andersen, L. H. Direct and Indirect Electron Emission from the Green Fluorescent Protein Chromophore. *Phys. Rev. Lett.* **2012**, *109*, 128101.

(18) Bochenkova, A. V.; Andersen, L. H. Photo-Initiated Dynamics and Spectroscopy of the Deprotonated Green Fluorescent Protein Chromophore. In *Photophysics of Ionic Biochromophores*; Brondsted Nielsen, S., Wyer, J. A., Eds.; Springer-Verlag: Heidelberg, 2013; pp 67−103.

(19) Mooney, C. R. S.; Horke, D. A.; Chatterley, A. S.; Simperler, A.; Fielding, H. H.; Verlet, J. R. R. Taking the Green Fluorescence Out of the Protein: Dynamics of the Isolated Gfp Chromophore Anion. *Chem. Sci.* **2013**, *4*, 921−927.

(20) West, C. W.; Hudson, A. S.; Cobb, S. L.; Verlet, J. R. R. Communication: Autodetachment Versus Internal Conversion from the S_1 State of the Isolated GFP Chromophore Anion. *J. Chem. Phys.* **2013**, *139*, 071104.

(21) Bochenkova, A. V.; Klaerke, B.; Rahbek, D. B.; Rajput, J.; Toker, Y.; Andersen, L. H. UV Excited-State Photoresponse of Biochromophore Negative Ions. *Angew. Chem., Int. Ed.* **2014**, *53*, 9797−9801.

(22) Deng, S. H. M.; Kong, X. Y.; Zhang, G. X.; Yang, Y.; Zheng, W. J.; Sun, Z. R.; Zhang, D. Q.; Wang, X. B. Vibrationally Resolved Photoelectron Spectroscopy of the Model Gfp Chromophore Anion Revealing the Photoexcited S-1 State Being Both Vertically and Adiabatically Bound against the Photodetached D-0 Continuum. *J. Phys. Chem. Lett.* **2014**, *5*, 2155−2159.

(23) Mooney, C. R. S.; Parkes, M. A.; Zhang, L. J.; Hailes, H. C.; Simperler, A.; Bearpark, M. J.; Fielding, H. H. Competition between Photodetachment and Autodetachment of the 2 $^1\pi\pi^*$ State of the Green Fluorescent Protein Chromophore Anion. *J. Chem. Phys.* **2014**, *140*, 205103.

(24) Kiefer, H. V.; Lattouf, E.; Persen, N. W.; Bochenkova, A. V.; Andersen, L. H. How Far Can a Single Hydrogen Bond Tune the Spectral Properties of the GFP Chromophore? *Phys. Chem. Chem. Phys.* **2015**, *17*, 20056−20060.

(25) West, C. W.; Bull, J. N.; Hudson, A. S.; Cobb, S. L.; Verlet, J. R. R. Excited State Dynamics of the Isolated Green Fluorescent Protein Chromophore Anion Following UV Excitation. *J. Phys. Chem. B* **2015**, *119*, 3982−3987.

(26) Kiefer, H. V.; Pedersen, H. B.; Bochenkova, A. V.; Andersen, L. H. Decoupling Electronic Versus Nuclear Photoresponse of Isolated Green Fluorescent Protein Chromophores Using Short Laser Pulses. *Phys. Rev. Lett.* **2016**, *117*, 243004.

(27) Bochenkova, A. V.; Mooney, C. R. S.; Parkes, M. A.; Woodhouse, J. L.; Zhang, L. J.; Lewin, R.; Ward, J. M.; Hailes, H.

C.; Andersen, L. H.; Fielding, H. H. Mechanism of Resonant Electron Emission from the Deprotonated GFP Chromophore and Its Biomimetics. *Chem. Sci.* **2017**, *8*, 3154−3163.
(28) McLaughlin, C.; Assmann, M.; Parkes, M. A.; Woodhouse, J. L.; Lewin, R.; Hailes, H. C.; Worth, G. A.; Fielding, H. H. Ortho and Para Chromophores of Green Fluorescent Protein: Controlling Electron Emission and Internal Conversion. *Chem. Sci.* **2017**, *8*, 1621−1630.
(29) Svendsen, A.; Kiefer, H. V.; Pedersen, H. B.; Bochenkova, A. V.; Andersen, L. H. Origin of the Intrinsic Fluorescence of the Green Fluorescent Protein. *J. Am. Chem. Soc.* **2017**, *139*, 8766−8771.
(30) Carrascosa, E.; Bull, J. N.; Scholz, M. S.; Coughlan, N. J. A.; Olsen, S.; Wille, U.; Bieske, E. J. Reversible Photoisomerization of the Isolated Green Fluorescent Protein Chromophore. *J. Phys. Chem. Lett.* **2018**, *9*, 2647−2651.
(31) Langeland, J.; Kjaer, C.; Andersen, L. H.; Nielsen, S. B. The Effect of an Electric Field on the Spectroscopic Properties of the Isolated Green Fluorescent Protein Chromophore Anion. *ChemPhysChem* **2018**, *19*, 1686−1690.
(32) Henley, A.; Fielding, H. H. Anion Photoelectron Spectroscopy of Protein Chromophores. *Int. Rev. Phys. Chem.* **2019**, *38*, 1−34.
(33) Bochenkova, A. V.; Andersen, L. H. Ultrafast Dual Photoresponse of Isolated Biological Chromophores: Link to the Photoinduced Mode-Specific Non-Adiabatic Dynamics in Proteins. *Faraday Discuss.* **2013**, *163*, 297−319.
(34) Voliani, V.; Bizzarri, R.; Nifosi, R.; Abbruzzetti, S.; Grandi, E.; Viappiani, C.; Beltram, F. Cis-Trans Photoisomerization of Fluorescent-Protein Chromophores. *J. Phys. Chem. B* **2008**, *112*, 10714−10722.
(35) Kaucikas, M.; Tros, M.; van Thor, J. J. Photoisomerization and Proton Transfer in the Forward and Reverse Photoswitching of the Fast-Switching M159t Mutant of the Dronpa Fluorescent Protein. *J. Phys. Chem. B* **2015**, *119*, 2350−2362.
(36) Klots, C. E. Temperatures of Evaporating Clusters. *Nature* **1987**, *327*, 222−223.
(37) Marsh, B. M.; Voss, J. M.; Garand, E. A Dual Cryogenic Ion Trap Spectrometer for the Formation and Characterization of Solvated Ionic Clusters. *J. Chem. Phys.* **2015**, *143*, 204201.
(38) Elliott, B. M.; Relph, R. A.; Roscioli, J. R.; Bopp, J. C.; Gardenier, G. H.; Guasco, T. L.; Johnson, M. A. Isolating the Spectra of Cluster Ion Isomers Using Ar-″Tag″ -Mediated IR-IR Double Resonance within the Vibrational Manifolds: Application to $NO_2^-\cdot H_2O$. *J. Chem. Phys.* **2008**, *129*, 094303.
(39) Voss, J. M.; Fischer, K. C.; Garand, E. Revealing the Structure of Isolated Peptides: IR-IR Predissociation Spectroscopy of Protonated Triglycine Isomers. *J. Mol. Spectrosc.* **2018**, *347*, 28−34.
(40) Wolke, C. T.; Menges, F. S.; Totsch, N.; Gorlova, O.; Fournier, J. A.; Weddle, G. H.; Johnson, M. A.; Heine, N.; Esser, T. K.; Knorke, H.; et al. Thermodynamics of Water Dimer Dissociation in the Primary Hydration Shell of the Iodide Ion with Temperature-Dependent Vibrational Predissociation Spectroscopy. *J. Phys. Chem. A* **2015**, *119*, 1859−1866.
(41) Støchkel, K.; Hansen, C. N.; Houmøller, J.; Nielsen, L. M.; Anggara, K.; Linares, M.; Norman, P.; Nogueira, F.; Maltsev, O. V.; Hintermann, L.; et al. On the Influence of Water on the Electronic Structure of Firefly Oxyluciferin Anions from Absorption Spectroscopy of Bare and Monohydrated Ions in Vacuo. *J. Am. Chem. Soc.* **2013**, *135*, 6485−6493.
(42) Xu, S.; Smith, J. E. T.; Weber, J. M. Hydration of a Binding Site with Restricted Solvent Access − Solvatochromic Shift of the Electronic Spectrum of a Ruthenium Polypyridine Complex, One Molecule at a Time. *J. Phys. Chem. A* **2016**, *120*, 7650−7658.

https://dx.doi.org/10.1021/acs.jpclett.0c00105
J. Phys. Chem. Lett. 2020, 11, 1940−1946